MECHANICAL, THERMAL AND TRIBOLOGICAL ASPECTS OF THE MACHINING PROCESS OF NODULAR IRON WITH COATED CARBIDE AND CERAMIC TOOLS

W. Grzesik, K. Żak

Summary

This paper overviews some typical cutting characteristics obtained in the turning of the pearlitic-ferritic nodular iron (EN-GJS-500-7 grade with UTS = 500 MPa) when using carbide tools coated with single TiAlN and multiple TiC/Ti(C,N)/Al_2O_3/TiN layers, as well as silicon nitride Si_3N_4 based ceramic tools. As a competitor, a P20 uncoated carbide grade was selected. The fundamental process readings include the cutting forces, the tool-chip interface temperature, Peclet number, friction coefficient and the tool-chip contact length as functions of cutting parameters. In particular, the measurements of cutting temperature were carried out using conventional tool-work thermocouple method and IR mapping technique. It is concluded based on many process characteristics that multilayer coated and ceramic tools can substantially improve the performance of nodular iron machining.

Keywords: Nodular iron, coated and ceramic tools, cutting temperature, tribological behaviour

Mechaniczne, cieplne i tribologiczne aspekty skrawania żeliwa sferoidalnego narzędziami z węglików spiekanych i ceramiki azotkowej z powłokami ochronnymi

Streszczenie

W pracy omówiono wybrane typowe charakterystyki procesu toczenia perlityczno-ferrytycznego żeliwa sferoidalnego (gatunek EN-GJS-500-7 o wytrzymałości na rozciąganie RM = 500 MPa). Stosowano ostrza z węglików spiekanych z naniesioną pojedynczą powłoką TiAlN lub wielowarstwową powłoką TiC/Ti(C,N)/Al_2O_3/TiN, a także ostrza z ceramiki azotkowej Si_3N_4. Węglik spiekany ISO P20 przyjęto jako materiał referencyjny. Prowadzono pomiary podstawowych wielkości procesu, składowych całkowitej siły skrawania, temperatury styku wiór-ostrze, liczby Pecleta, współczynnika tarcia, długości styku wiór-ostrze w funkcji parametrów skrawania. Pomiary temperatury skrawania prowadzono metodą termoelementu naturalnego i metodą pirometrii w podczerwieni IR. Uzyskane charakterystyki procesu wskazują, że zastosowanie ostrzy z węglików spiekanych z powłokami wielowarstwowymi i ceramiki azotkowej polepsza istotnie wydajność procesu skrawania żeliwa sferoidalnego.

Słowa kluczowe: żeliwo sferoidalne, pokrywane narzędzia z powłokami wielowarstwowymi i ceramiczne, temperatura skrawania, właściwości tribologiczne

Address: Prof. W. GRZESIK, K. ŻAK, Ph.D. Eng., Dept. of Manufacturing Engineering and Production Automation, Opole University of Technology, 45-271 Opole, 5th Mikolajczyka St., Poland, E-mail: w.grzesik@po.opole.pl, k.zak@po.opole.pl

1. Introduction

In recent years the development of new cast iron materials has been seen to offer a greater competition to other materials and make cast iron a competitor for components not traditionally manufactured from this material [1]. In particular, the two materials with significantly higher strengths in comparison to classical grey cast irons are Compacted Graphite Iron (CGI) and Austempered Ductile Iron (ADI). Their excellent mechanical and fatigue strengths result from lamellar (vermicular) graphite and globular graphite structures respectively [1, 2].

Exemplarily, the increasing use of GGV/CGI vermicular/compact graphite iron as a suitable material for engine blocks in high performance diesel engines to meet rigorous eco-standards is reported [2, 3]. Basically, they originated from the necessity of designing lighter and dimensionally smaller car engines with higher power trains, in comparison to engines manufactured using traditional materials such as Al-Si alloys or grey cast irons [1].

The inspirations of the experimental study when machining nodular irons are sourced in the promising statistics from automotive industry which report substantially growing use of cast irons, not only previously mentioned Compacted Graphite Iron (CGI) and Austempered Ductile Iron (ADI), but also ductile nodular iron. On the other hand, machining the range of grey and ductile irons is complicated by the fact that these materials can vary in machinability so greatly, often within the same batch [4]. In addition, the data which quantified the machining process of nodular cast iron practically are not available in the metal cutting literature. More data can be found for different grades of grey cast irons machined with different tools such as white (oxide) and silicon nitride ceramics [5]. It is reported that for a GG 25 cast iron machined with nitride ceramic tools the cutting temperature measured by means of IR technique was lower of about 90-120 ^{0}C than for oxide ceramic tools (610 vs. 730 ^{0}C for Al_2O_3/ZrO_2 and 700 ^{0}C for Al_2O_3/TiCN ceramics) under the same cutting parameters (v_c = 500 m/min, f = 0.32 mm/rev, a_p = 2 mm). Apart from the pure oxide (Al_2O_3) and mixed ceramics (Al_2O_3 + TiC) both silicon nitride (sialon) and cubic boron nitride (pCBN) have also found increasing applications [6]. The tool-life tests performed on the pearlitic iron bars with sialon indicated low cratering, which can capitalise this material due to its toughness.

The experimental research carried out is focused on the mechanical, thermal and contact processes occurring in machining of a nodular EN-GJS iron when using TiAlN and TiC/Ti(C,N)/Al_2O_3/TiN coated carbide and silicon nitride Si_3N_4 based ceramic tools. The process behaviour is based on the fundamental process readings including forces, cutting temperature and heat transfer condition as well as friction coefficient and tool-chip contact length.

2. Experimental details

2.1. Characterization of tested material

In general, there are three possible types of microstructures of ductile cast-irons, namely: ferritic, pearlitic and pearlitic-ferritic nodular irons with graphite nodules size varying between 20 and 60 μm. In this study the pearlitic-ferritic nodular iron containing approximately 50% pearlite, 40% ferrite and 10% graphite was chosen as the workpiece material.

The mechanical properties of machined nodular iron are listed in Table 1. In particular, this material has the ultimate tensile strength of UTS = 500 MPa and the measured average hardness of about 175 HB (indicated by a star marker in Table 1). Bars of the maximum 100 mm in diameter, which were primarily machined under roughing and finishing conditions, were used.

Table 1. Mechanical properties of tested material [7]

Symbol	UTS MPa	Y MPa	Elongation A %	Hardness HB
EN-GJS-500-7	500	320	7	170-230 175* *measured value

2.2. Cutting tools and machining conditions

Cutting tool configuration of ISO-TGNR 2020-16 type was used and tips with plane rake face of ISO-TNMA 160408 type were selected.

Three different carbide tools were tested: conventional ISO-P20 sintered carbide as a reference, coated with single TiAlN layer deposited by Teer Ltd (UK) and commercial NTH1 mulilayer grade CVD-TiC/Ti(C,N)/Al_2O_3/TiN by Sandvik-Baildonit, Poland. In addition, silicon nitride Si_3N_4 based ceramic tools of a CC 6090 grade by Sandvik Coromant were included into machining tests. Cutting parameters and selected cutting tool angles are listed in Table 2.

Table 2. A set of cutting conditions used in the study

Cutting speed, m/min	Feed rate, mm/rev	Depth of cut, mm	Cutting tool geometry
1st series 160-315	0.16	2	$\kappa_r = 90°, \alpha_o = 5°,$ $\gamma_o = -5°, \lambda_s = -6°$
2nd series 270 for P20 190	0.04, 0.08, 0.1, 0.16, 0.2, 0.28		

Two series of longitudinal turning trials, first with variable cutting speed and second with variable feed rate were included into the experimental program. All trials were repeated, each for three-times.

2.3. Experimental techniques and process characteristics

Measured signals of the cutting forces and the tool-chip temperature (the *emf* signals) were recorded and analyzed in the on-line mode by means of appropriate data acquisition system. Additionally, the IR thermal mapping technique was employed (Fig. 1) to register thermal fields occurring during nodular iron machining with silicon nitride cutting tips. The chip and the workmaterial can be considered as a thermally homogeneous material, so that the material thermal picture of the chip is comparable to the temperature map in the median plane owing to the assumption of 2D cutting, as shown in Ref. [8]. In this step of experimentations a CCD-infrared camera was applied to obtain a thermal map of tool-chip-workmaterial system. The temperature measurement range is from 500 to 1000°C, which corresponds to the CCD sensor capacity and the settings (diaphragm position, infrared filters) used for the camera during the tests. This limit is fixed by the near infrared wavelength domain and the signal/noise ratio of electronic acquisition (3.4 – 5 μm wavelength interval). The observation area was 2 × 2 mm. The spatial resolution of the system is around 12 μm. The acquisition rate was 2 images per second.

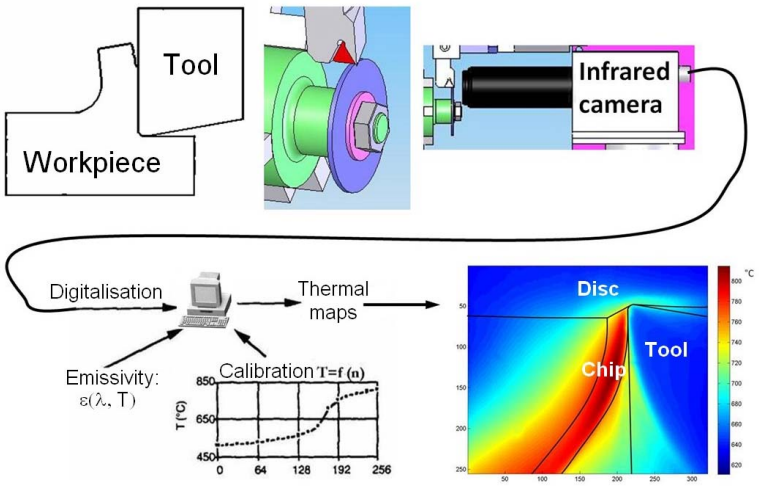

Fig. 1. A scheme of IR thermal mapping technique [9]

The calibration of the IR-CCD system was done against a black body cavity for which temperature was carefully controlled (resolution ± 1°C). The operating temperature range was between 500-1000°C. For each temperature, a thermal map was recorded by step of 25°C in order to calculate the average grey level intensity of the image. The equation between the temperature of the black body as a function of grey level was obtained from different integration times. The

characterization of the emissivity of the work material has been made by heating the work material at various temperatures in a furnace with an inert gas so as to avoid any oxidations of steel. A thermocouple has been sticked on the face observed by the camera so as to correlate the real temperature and the measurements made by the camera. This step necessitates the integration of the Planck's radiation law. Since no primitive of this equation is known, the Gauss point method has been used so as to have the direct relation between the luminance of the black body and the temperature.

On the other hand, the tool-chip contact images recorded by a CCD camera were digitized and processed in order to extract the sharp boundary line between abrasively worn and unworn zones on the tool rake face (see Fig. 7). Subsequently, the tool-chip contact length was determined using computerized dimensioning system described in Ref. [10].

Based on the experimentally determined values of the tool-chip contact length for all material couples the Peclet number was calculated using the formulae [10, 11]:

$$Pe_c = \frac{v_{ch} l_{nc}}{\alpha_w} \tag{1}$$

where v_{ch} is the chip velocity, l_{nc} is the natural tool-chip contact length and α_w is the thermal diffusivity of the workpiece material. The value of thermal diffusivity for the nodular cast iron being machined was taken at 1.184×10^{-5} m^2/s. It should be noted that heat transfer to the stationary element is less intensive for larger values of Peclet number [11].

The coefficient of friction was calculated as the ratio of the friction force F_γ to the normal force acting on the rake face $F_{\gamma N}$. Forces F_γ and $F_{\gamma N}$ were computed after simple resolving of the active force F_a using the Merchant's circle technique [12].

3. Experimental details and discussion

3.1. Cutting forces

Figure 2 shows changes of the measured values of the cutting force for all tested cutting tools when varying cutting speed (Fig. 2a) and feed rate (Fig. 2b). As illustrated in Fig. 2a higher cutting forces were consequently recorded for silicon nitride ceramic tools for which the F_c force decreases slightly from 810 to 740 N when cutting speed increases from 160 up to 320 m/min. On the other hand, lower cutting forces were measured for multilayer coated tools for which minimum friction coefficient was computed (see Fig. 9). But for the latter case

F_c force does not decrease visibly but varies of about 600±20N. In general, the cutting force elevates visibly with the increase of feed rate for both cutting tools tested. For example, for Si_3N_4 tools F_c increases from 300 for f = 0.04 mm/rev to above 1060 N for feed of 0.28 mm/rev.

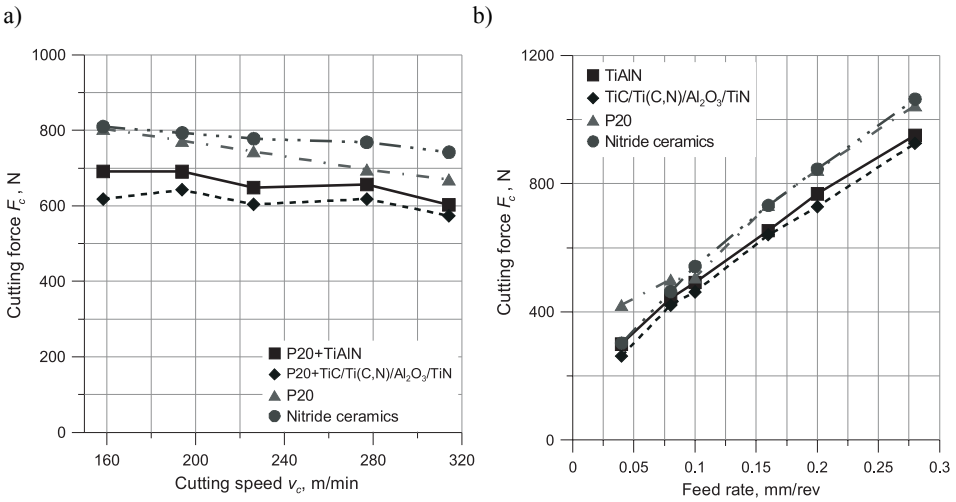

Fig. 2. Changes of the cutting force for variable cutting speed (a) and feed rate (b)

The trend in changes of the feed force with variable cutting speed shown in Fig. 3a is similar to that shown in Fig. 2a and the values of F_f force for coated carbide tools are, in principal, lower about 200 N than corresponding cutting forces measured for Si_3Ni_4- based tools. The rise of the feed force due to the increase of feed rate (Fig. 3b) is pronounced and ranges from 230 to 380 N and 310 to 630 N for multilayer coated carbide and Si_3Ni_4- based tools, respectively.

3.2. Thermal characterization of tool-chip interface

Plot showing changes in the contact temperature for different natural thermocouple combinations is presented as the function of cutting speed in Fig. 4. In general, in the machining tests performed cutting temperature varies between 370 and 550^0C depending on the cutting tool material and cutting conditions employed. In general, the contact temperatures are lower than in machining AISI 1045 carbon steel due to limited heat generation in the deformation source (mainly small discontinuous chips were formed).

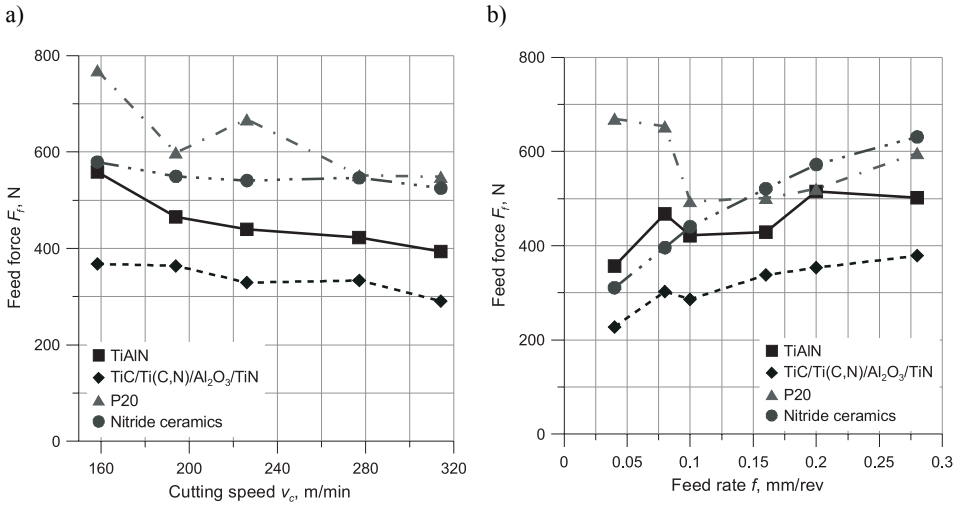

Fig. 3. Changes of the feed force for variable cutting speed (a) and feed rate (b)

As shown in Fig. 4, higher interface temperatures, above 140 and 60^0C in comparison to the P20 and four-layer coated carbides, occur at highest speed of 315 m/min when coupling TiAlN coated carbide with pearlitic-ferritic nodular iron. This can be referred to more severe adhesion interaction between sliding materials confirmed by the observations of wear patterns and partial destruction of coating. As reported in Ref. [13], the friction coefficient for the TiAlN-steel

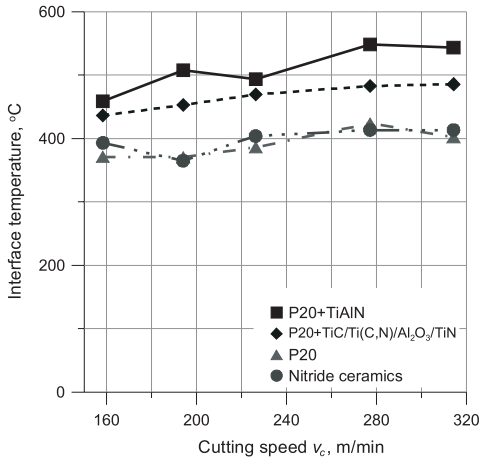

Fig. 4. Influence of cutting speed on average interface temperature.
Cutting condition: v_c = 160-320 m/min, f = 0.16 mm/rev

pair is relatively high and based on the current experiments it reaches about 0.55. Also, as shown in Fig. 8b, in this case the contact length (area) is substantially lower than for the two references. In general, the increase of the cutting temperature due to increase of the cutting speed from 160 to 315 m/min, documented in Fig. 4, is surprisingly low (only about 35-70^{0}C). More regular, quite monotonic increase of the interface temperature can be observed for multilayer coated tools.

Figures 5 and 6 characterize the heat transfer effectiveness in the machining of nodular cast iron in terms of the values of Peclet number calculated for all cutting tool materials using Eqn. (1). It is clear from Fig. 5 that all three carbide-based tools indicate similar heat transfer conditions for a constant cutting speed , i.e. the same heat partition to the chip, whereas according to Fig. 6, the silicon nitride ceramic tools cause the larger portion of heat to be transferred to the tool. This is because the thermal conductivity of Si_3N_3 material at lower temperatures is high enough to cumulate more heat in the tool body [10]. Probably, this fact explains some tendency towards cratering when machining cast irons, reported earlier in Ref. [8]. On average, Peclet numbers determined for nitride ceramic tools are 2-3 times lower than for other carbide-based tools tested. Better heat transfer conditions are observed at higher cutting speeds; for example at v_c = 320 m/min, Pe_c = 130 and 50 for the four-layer coated carbide and silicon nitride ceramics tools.

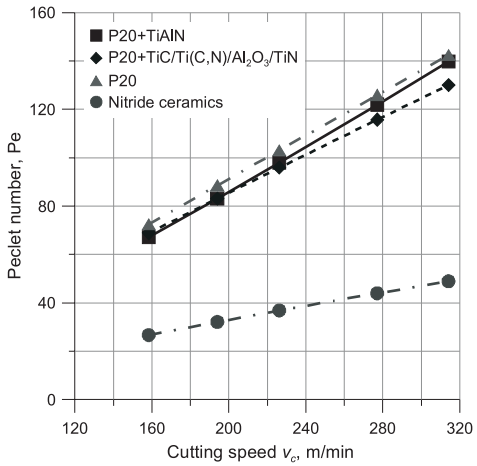

Fig. 5. Influence of cutting speed on Peclet number.
Cutting condition: v_c = 160-320 m/min, f = 0.16 mm/rev

Figure 6 depicts more visibly that coated tools coupled with nodular cast iron perform better at higher temperature, i.e. the same values of Peclet number

are determined at different contact temperatures. This fact also confirms the vital role of the thermal properties (the thermal conductivity or heat capacity) in creating the optimal heat transfer conditions for a given tool-workpiece pair.

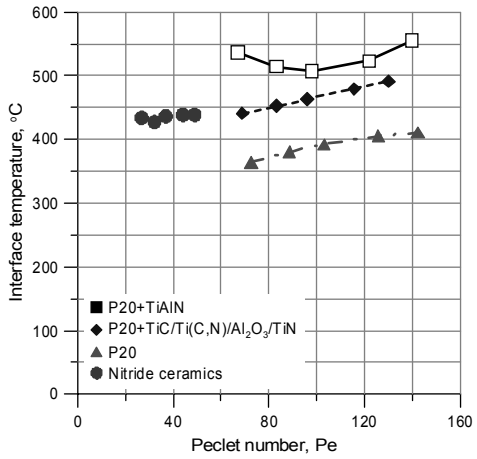

Fig. 6. Interface temperature vs. Peclet number.
Cutting condition: v_c = 160-320 m/min, f = 0.16 mm/rev

3.3. Mechanical characterization of tool-chip contact

Figure 7 illustrates the planimetry technique of the digitized tool-chip contact image applied for determining the contact area and the contact length. In case shown in Fig. 7, the average contact length for the depth of cut of 2 mm was estimated to be equal to 0.305 mm.

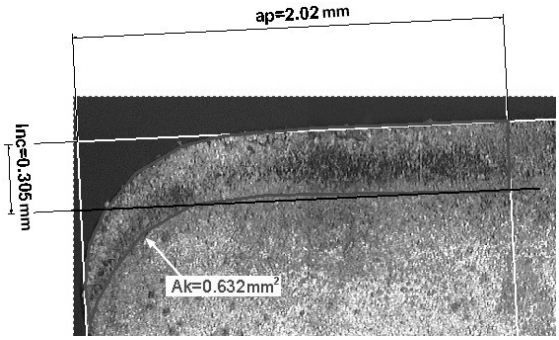

Fig.7. Exemplary estimation of the contact length from contact image for a four-layer coating (average value of l_{nc} = 0.305 mm was treated as representative).
Cutting condition: v_c = 190 m/min, f = 0,16 mm/rev, a_p = 2 mm

The frictional conditions developing on the tool rake face result from the dimensions of the contact between the tool and the chip, especially at lower feeds. Fig. 8a shows that cutting tool material is one of the decisive factors influencing the tool-chip length/area. It should be seen from Fig. 8a that for a reference feed of 0.16 mm/rev the value of l_{cn} varies from 0.115 mm for Si_3N_4 ceramics to 0.35 mm for P20 uncoated carbide tools. As expected the highest values of the contact length were recorded for maximum feeds employed. On the other hand, it was revealed that cutting speed practically does not influence the contact area/length. For comparison, Fig. 8b illustrates the relationship between the contact areas (lengths) for a C45 carbon steel and pearlitic-ferrlitic nodular cast iron machined and the range of feed rates. A unique phenomenon occurs which causes that for plastic workpiece materials the contact area increases distinctly with the increase of feed rate, whereas for nodular cast iron the relevant maximum changes are only about 30%. Moreover, probably local plastic deformation of the chip material causes that below the feed rate of 0.08 mm/rev the contact area for a C45 steel is lower than for nodular cast iron.

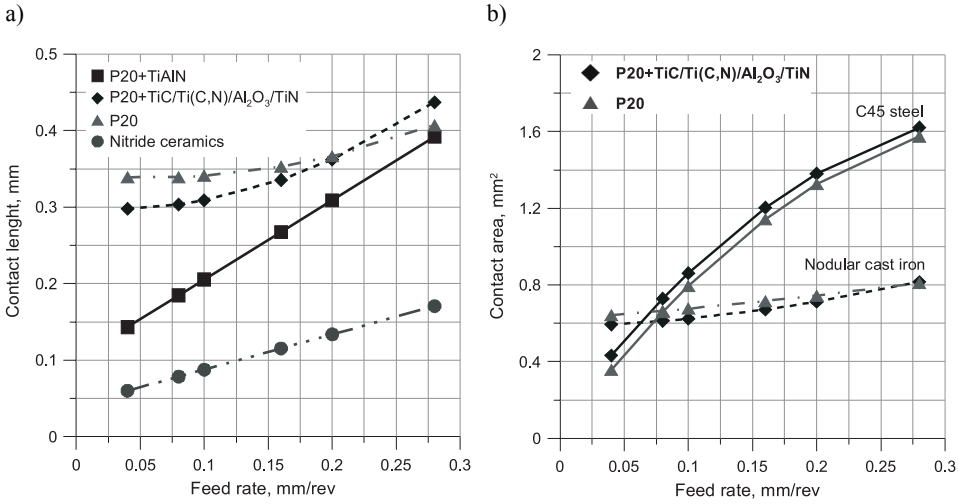

Fig. 8. Influence of feed rate on the tool-chip contact length (a) and contact area including C45 carbon steel (b). Cutting speed: v_c = 270 m/min and v_c = 190 m/min for P20 tools

As shown in Figs. 9 (a) and (b) cutting tool material changes visibly the tribological conditions at the tool-chip interface. When varying the cutting speed, see Fig. 9a, multi-layer coated tools produced the lowest friction, and the appropriate values vary slightly around 0.4 and 0.55 for multilayer and TiAlN coatings respectively. The highest values of μ of 0.65-0.8 were recorded for uncoated P20 carbide tools (the maximum values of 1.3 were obtained for the

minimum feed of 0.04 mm/rev which suggests rather strong adhesive interaction). When varying feed rate, as in Fig. 9b, the μ value of about 0.3 was determined for TiC/Ti(C,N)/Al_2O_3/TiN coated tools and the maximum feed rate of 0.28 mm/rev. This results from the substantial increase of the normal force $F_{\gamma N}$, as assessed by computations up to 950 N, whereas for feed of 0.16 mm/rev the $F_{\gamma N}$ was equal to 670 N. In contrast, severe friction with μ values of 1.0-1.3 exists for both uncoated carbide and TiAlN tools.

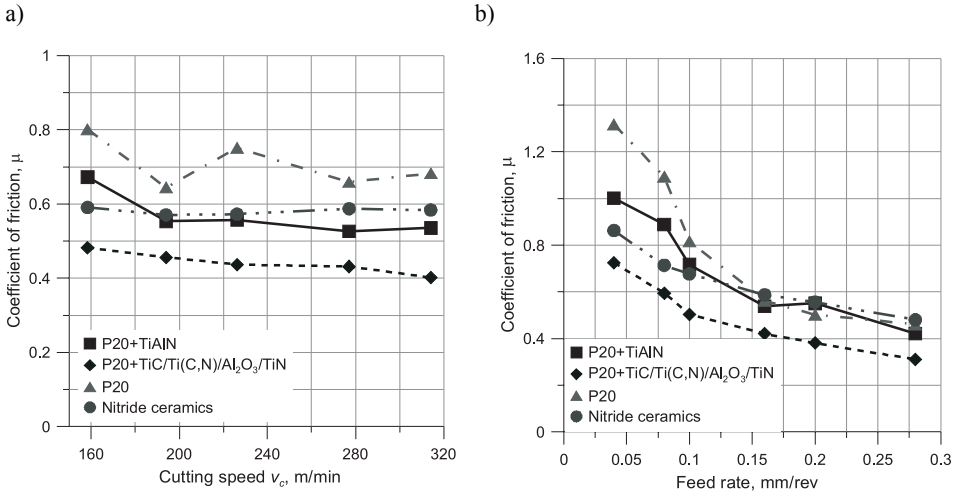

Fig. 9. Influence of cutting speed (a) and feed rate (b) on the coefficient of friction. Cutting condition: v_c = 160-320 m/min, f = 0.16 mm/rev (a) and v_c = 270 m/min, f = 0.04÷0.28 mm/rev for P20 v_c = 190 m/min (b)

4. Conclusions

1. It was revealed that we can change the tool-chip contact conditions when machining of nodular cast iron with coated carbide and silicon nitride ceramic tools. In particular, they concern such contact characteristics as the interface temperature, contact length and friction intensity.

2. Higher interface temperatures, for example above 140 and 80^0C at highest speed of 315 m/min in comparison to P20 uncoated carbide tools, occur for TiAlN and four-layer coated carbides respectively. This fact can be discussed in terms of different thermal conductivities of cutting tool materials. In contrast, cutting temperatures for silicon nitride ceramic tools, measured by means of a CCD infrared camera are practically matched those recorded for conventional P20 carbide tools.

3. Coated tools coupled with nodular cast iron perform better at higher temperature, i.e. they produce higher values of Peclet number in comparison to uncoated carbide tools. Moreover, Si_3N_4 ceramic tools provide visibly lower, 2-2.5 times lower, values of Peclet number.

4. As documented, cutting tool material influences the tool-chip length/area in such a way that exemplarily for a reference feed of 0.16 mm/rev the value of l_{cn} varies from 0.115 mm for Si_3N_4 ceramics to 0.35 mm for P20 uncoated carbide tools. Hence, the lowest contact lengths were recorder for silicon nitride ceramic tools.

5. Due to different chip formation mechanisms (discontinuous versus continuous) the contact lengths for nodular cast iron are, at higher feeds, distinctly lower than for a C45 carbon steel and the same tool materials.

6. In the machining of nodular cast iron multi-layer coated tools produced the lowest friction. For instance, the μ value of about 0.3 was determined for TiC/Ti(C,N)/Al_2O_3/TiN coated tools and the cutting speed of 270 m/min, keeping the maximum feed rate of 0.28 mm/rev. In sharp contrast, μ exceeds 1, as for example for uncoated carbide tools and feed of 0.04 mm/rev it approaches 1.3.

References

[1] H. SCHULZ, U. REUTER: Verschleißmechanismus geklärt: GGV-Motoren reif für die Großserie. *Werkstatt und Betrieb*, **134**(2001)7-8, 80-82.
[2] G. BYRNE, D. DORNFELD, B. DENKENA: Advancing cutting technology. *Annals of CIRP*, **52**(2003)2, 483-507.
[3] F. J. MOMPER: Neue Schneidstoffe für neue Werkstoffe. *Werkstatt und Betrieb.* **131**(1998)5, 390-394.
[4] D. Graham: Machining cast iron. *Manufacturing Engineering*, **136**(2006)2.
[5] H. K. TÖNSHOFF, B. DENKENA: Temperaturbeanspruchung keramischer Schneidstoffe bei unterbrochenem Schnitt. *VDI-Z*, **132**(1990)6, 60-64.
[6] D. K. ASPINWALL, W. CHEN: Machining of grey cast iron using advanced ceramic tool materials. Proc. 27th Matador Conference, Manchester 1988, 225-230.
[7] Nodular iron. Classification. Polish and European Standard PN-EN 1563:2000.
[8] R. M'SAOUBI, H. CHANDRASEKARAN: Investigation of the effects of tool micro-geometry and coating on tool temperature during orthogonal turning of quenched and tempered steel. *Journal of Machine Tools and Manufacture*, **44**(2004), 213-224.
[9] W. GRZESIK, J. RECH, K. ZAK, C. CLAUDIN: Machining performance of pearlitic-ferritic nodular cast iron with coated carbide and silicon nitride cutting tools. *Journal of Machine Tools and Manufacture*, **49**(2009)2, 125-133.
[10] W. GRZESIK: The influence of thin hard coatings on frictional behaviour in the orthogonal cutting process. *Tribology International*, **33**(2000), 131-140.

[11] W. GRZESIK, P. NIESLONY: A computational approach to evaluate temperature and heat partition in machining with multilayer coated tools. *Journal of Machine Tools and Manufacture*, **43**(2003), 1311-1317.
[12] W. GRZESIK: Advanced machining processes of metallic materials. Elsevier, Amsterdam 2008.
[13] W. GRZESIK: *Advanced Protective Coatings for Manufacturing and Engineering*, Hanser Gardner Publ., Cincinnati 2003.

Received in February 2009